Hydrogen-Release Mechanisms

DOI: 10.1002/anie.200702886

Catalyzed Dehydrogenation of Ammonia–Borane by Iridium Dihydrogen Pincer Complex Differs from Ethane Dehydrogenation**

Ankan Paul and Charles B. Musgrave**

Onboard hydrogen storage will play a critical role in a hydrogen-based fuel economy.[1] Ammonia–borane (AB, NH_3BH_3) can potentially store a significant percent of hydrogen chemically, motivating an intense effort to investigate its potential application as an onboard hydrogen-storage system.[1] This approach involves low-temperature release of hydrogen from ammonia–borane and subsequent regeneration. Considerable progress has recently been made in developing catalytic systems that can dehydrogenate amine–boranes.[2–9] Goldberg et al. have shown that room-temperature dehydrogenation of AB can be achieved at an appreciable rate using the catalytic iridium pincer complex, $[(POCOP^{tBu})Ir(H)_2]$ (**1**), where $POCOP^{tBu} = \eta^3$-1,3-$(OPtBu_2)_2C_6H_3$.[6] Compound **1** belongs to a class of traditional catalysts for alkane dehydrogenation and transfer dehydrogenation.[10–16] The isoelectronic and structural similarity of C_2H_6 to AB inspired the use of iridium pincer complexes for the dehydrogenation of AB.

The dehydrogenation of alkanes by iridium pincer complexes has been suggested to proceed through catalyst dehydrogenation followed by oxidative C–H addition.[10–13,17,18] Furthermore, pathways involving oxidative C–H addition on the native hydrogenated form of the iridium catalyst have also been suggested.[10–13] Because AB has a heteroatomic backbone, additional pathways are possible, as the reaction can proceed by B–H or N–H bond activation. It is generally believed that transition-metal-catalyzed AB dehydrogenation initiates through oxidative B–H activation at the transition-metal center followed by β-H elimination from the N–H bond. Herein, we report a theoretical study of the mechanism of ammonia–borane dehydrogenation using a prototype iridium pincer catalyst, $[(POCOP^{Me})Ir(H)_2]$ (**2**).[7,8]

Molecular geometries were optimized using B3LYP within GAUSSIAN 03 with basis set B1 (Ir: LANL2DZ, other atoms: 6-31 + G**).[19] Single-point energies were computed using the CPCM[20] solvent model to account for solvent effects from THF used in the actual reaction, with basis sets B1 and B2 (Ir: LANL2DZ, with re-optimized 6p functions, a set of f polarization functions, exponent = 0.938, and diffuse d functions, exponent = 0.07).[10] Zero-point energies were computed in the gas phase at the B3LYP/B1 level of theory. We report the solvent-phase energies including zero-point energy contributions at the B3LYP(CPCM)/B2//B3LYP/B1 level of theory. Additional calculational details are provided in the Supporting Information.

Pathways by which AB may be dehydrogenated were then theoretically predicted. The THF solvent may directly coordinate to the iridium catalyst; Brookhart et al. have recently shown by NMR-spectroscopic proton–proton coupling studies that a chlorine atom of CH_2Cl_2 used as solvent can coordinate to the iridium center of complex **1**.[21] Alternatively, our computations predict that AB can coordinate to the iridium center of both the original catalyst **1** or of prototype **2** through a hydrogen atom with hydride character on the boron end of AB. Intermediate **6** (shown in Scheme 1 is thus formed from the adduct of AB and **2**. Shimoi et al. have reported analogous coordination by B–H bonds with hydride character to transition-metal centers.[22] Formation of **6** is energetically favored by 10.2 kcal mol^{-1}. In contrast, the adduct formed between **1** and THF will be less stable than that of **1** and AB, as the bulky *tert*-butyl groups on phosphorus atoms neighboring the iridium center hinder coordination of larger molecules (such as THF compared to AB). Thus, we consider intermediate **6** as a reference point for computing our energetic barriers. Our computational investigations uncovered two distinct pathways for AB dehydrogenation. One path, the Ir^{I} path, involves dehydrogenation of AB by a 14e$^-$ iridium intermediate (Scheme 1) whereas the other, the

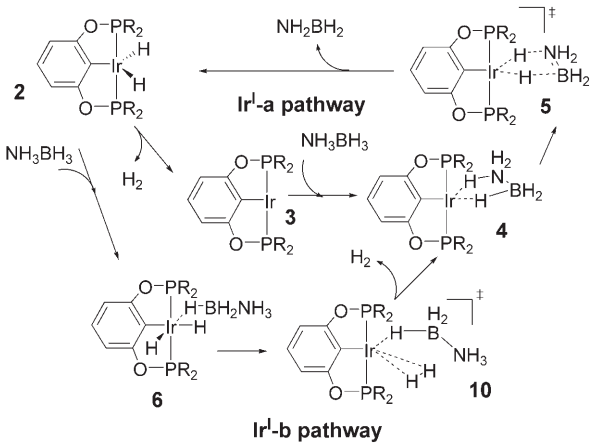

Scheme 1. Dehydrogenation pathways Ir^{I}-a (**2**–**3**–**4**–**5**–**2**) and Ir^{I}-b (**2**–**6**–**10**–**4**–**5**–**2**) for AB dehydrogenation. R = methyl.

[*] Dr. A. Paul, Prof. Dr. C. B. Musgrave
Department of Chemical Engineering
Keck Science Building, Stanford University
Stanford, CA-94305 (USA)
E-mail: ankan@stanford.edu
chasm@stanford.edu

[**] A.P. would like to thank Paul Zimmerman for help in editing the draft. A.P. and C.B.M. would like to thank Pittsburgh Supercomputing Center for a Computational Time Grant.

Supporting information for this article is available on the WWW under http://www.angewandte.org or from the author.

Ir^{III} path, proceeds through a $16e^-$ iridium intermediate (Scheme 2).

In the Ir^I path, prototype **2** transforms to the $14e^-$ intermediate **4** (pathways Ir^I-a and Ir^I-b, Scheme 1). In

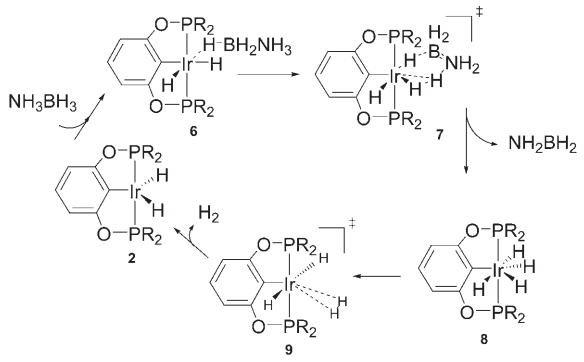

Scheme 2. Ir^{III} pathway (**2**–**6**–**7**–**8**–**9**–**2**) for AB dehydrogenation. R = methyl.

pathway Ir^I-a for **2**, we were unable to locate a transition state (TS) corresponding to the dehydrogenation, indicating that the reverse reaction, hydrogenation of the iridium center, is barrierless. Krogh-Jespersen et al. reported similar findings for dehydrogenation of analogous iridium catalysts.[10,11] The dehydrogenation energy of **2** (Figure 1) is 15.7 kcal mol^{-1} in THF (19.2 kcal mol^{-1} without zero-point correction) and 25.9 kcal mol^{-1} above intermediate **6**. This value for **2** differs substantially from the gas-phase dehydrogenation energy (without zero-point correction) of 31.7 kcal mol^{-1} reported earlier by Krogh-Jespersen et al.[10] Our calculated gas-phase dehydrogenation energy for **2** (29.5 kcal mol^{-1}) essentially reproduces the reported value, and suggests that in the gas phase, the energy of dehydrogenation is prohibitively high.

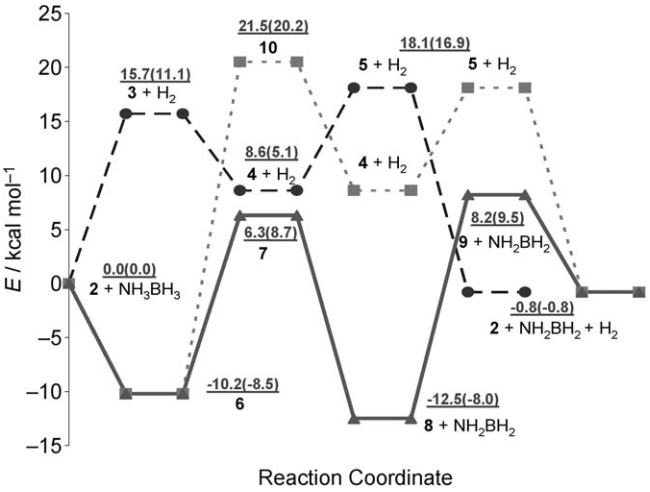

Figure 1. Total energy (ΔE) profiles in kcal mol^{-1} for pathways Ir^I-a (circles, long dashes), Ir^I-b (squares, short dashes) and Ir^{III} (triangles, lines) of the catalytic dehydrogenation of ammonia–borane in THF. Relative energies are calculated using B3LYP(CPCM)/B2//B3LYP/B1 with zero-point correction. Relative energies calculated with B3LYP-(CPCM)/B1//B3LYP/B1 are shown in parentheses.

Polar solvents can have substantial effects on reaction energies, and our computed dehydrogenation energies in different solvents and in vacuum (see Supporting Information) demonstrate that dehydrogenation energies of **2** are significantly lower in polar solvents compared to those in nonpolar media and gas phase.

Though C–H activation of alkanes is widely known for Ir^I, we were unable to identify an N–H- or a B–H-activation transition state at the dehydrogenated iridium center of species **3**.[10–13,17,18] The dehydrogenated iridium complex can however remove two hydrogen atoms in a concerted fashion from the NH_3BH_3 Lewis acid–base adduct via a five-membered TS **5** (see Scheme 1 and Figure 2a), which lies 18.1 kcal mol^{-1} above the starting reactants. We were unable to locate an analogous TS for concerted ethane dehydrogenation, suggesting that this pathway is not available for alkanes.

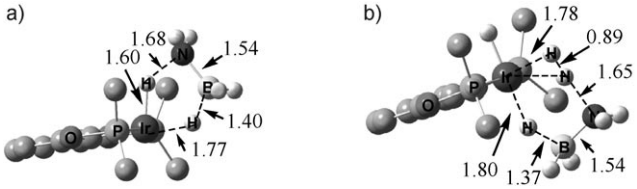

Figure 2. B3LYP-optimized molecular geometries of a) five-membered (**5**) and b) six-membered transition states (**7**) for concerted dehydrogenation of NH_3BH_3. Selected calculated bond lengths [Å] are indicated. Hydrogen atoms attached to carbon are omitted for clarity.

Transformation of **2** to intermediate **4** can also occur by formation of intermediate **6** and subsequent dehydrogenation through TS **10** (pathway Ir^I-b, Scheme 1). Since formation of intermediate **6** is barrierless and significantly exothermic, it is likely AB molecules will rapidly coordinate to the catalytic species. Adduct **6** could transform to intermediate **4** through TS **10**, but this TS lies 31.7 kcal mol^{-1} above **6**, making this barrier prohibitively high at room temperature. Similarly, dehydrogenation transition state **5** lies 28.3 kcal mol^{-1} above intermediate **6**. Consequently, pathways Ir^I-a and Ir^I-b are predicted to be inactive at room temperature (Figure 1). However, pathways involving TS **5** may be relevant to recently reported work by Baker et al. on AB dehydrogenation by nickel carbene catalysts.[7] This catalytic cycle is currently under investigation.

An alterative route for dehydrogenation of **6** proceeds by six-membered TS **7** (Figure 2b) on the Ir^{III} pathway (Scheme 2). This route corresponds to a concerted transfer of hydride from boron to the iridium center (analogous to B–H activation as in Reference [23]), and a simultaneous transfer of a proton from the nitrogen end to a hydride bound to the iridium center. The six-membered TS **7**, which leads to the formation of intermediate **8**, $[(POCOP^{Me})Ir(H)_4]$, lies 16.5 kcal mol^{-1} above intermediate **6** and 6.3 kcal mol^{-1} above the reactants. Species **8** subsequently undergoes further dehydrogenation through TS **9** and regenerates **2** in the process. Our computations indicate that intermediate **8** is the most stable intermediate formed in the catalytic cycle. Transition states **7** and **9** are predicted to lie 18.8 and

20.7 kcal mol^{-1} above intermediate **8**. TS **7** is slightly less stable than TS **9**, but the difference in stability falls within the error range of the computational method used. Hence, it is likely that this catalytic process has two barriers which determine the rate of the reaction. The Ir^{III} pathway is predicted to be the catalytic pathway for AB dehydrogenation, with a rate-limiting barrier of 20.7 kcal mol^{-1}. The high barrier to regeneration of **2** from the most stable intermediate **8** soundly explains the observation of the analogous [(POCOP^{tBu})Ir(H)$_4$] as the major intermediate immediately after the reaction is started.[6] Figure 1 illustrates the potential energy profiles of the catalytic pathways; additional pathways with high-barrier N–H activation at **2** are provided in the Supporting Information.

The contrasting electronic structure of C_2H_6 and AB is emphasized by their differing low-barrier dehydrogenation pathways by iridium pincer complexes. Both pathways for AB involve concerted removal of hydrogen atoms, which is not observed for its isoelectronic analogue ethane. This dichotomy arises from the dissimilar natures of the hydrogen atoms of AB and C_2H_6. In AB the amine can act as a proton donor and borane as a hydride donor, whereas the absence of polarity in alkanes precludes this behavior. The Mulliken charge on each hydrogen on the amine is +0.19 e, indicating their protonic nature. The hydrogen atoms of the borane are negatively charged (−0.25 e) and hence the borane end behaves like a hydride. The HOMO of intermediate **6** (see Figure 3) has significant Ir d_{xz} character and substantial s character for the equatorial hydride bound to iridium, and the LUMO has substantial Ir d_{z^2} character. For ammonia–borane dehydrogenation the proton of the amine is transferred to the hydride bound to iridium and LUMO d_{z^2} orbital accepts a hydride from the boron end. The frontier orbitals of **3** (see Supporting Information) play a similar role in the dehydrogenation of AB along the alternative Ir^{I} pathway.

After NH_2BH_2 is formed, it is likely to polymerize in the THF solvent. Preliminary studies show that a THF-catalyzed linear dimerization has a barrier of only 8.9 kcal mol^{-1}, which may explain the rapid initiation of polymerization (see Supporting Information). The polymerization pathways are currently under investigation. Pentamer formation (as a major product) has been reported in other processes.[24] It is known that the trimer is soluble in ethers and so may be formed in the reaction medium transiently, while the pentamer is insoluble and precipitates out of the reaction medium displacing the equilibrium towards more pentamer formation. Goldberg et al. reported the formation of the pentamer on analysis of the solid formed in the reaction media during iridium pincer catalyzed dehydrogenation of AB.[6] It is not likely that the catalyst plays a role in the assembly of the pentameric cycloborazane as the iridium center of the catalyst is sterically hindered owing to the presence of the bulky *tert*-butyl groups on the neighboring phosphorus atoms.

In summary, we have shown that AB dehydrogenation proceeds through a concerted removal of hydrogen by iridium pincer catalysts. This process differs from the dehydrogenation of ethane, which involves C–H oxidative addition, despite AB being isoelectronic to ethane. The concerted mechanism stands in contrast to the recently predicted mechanism of titanocene dehydrogenation of amine–boranes by Ohno and Luo which involves a stepwise mechanism which is initiated by N–H activation.[25]

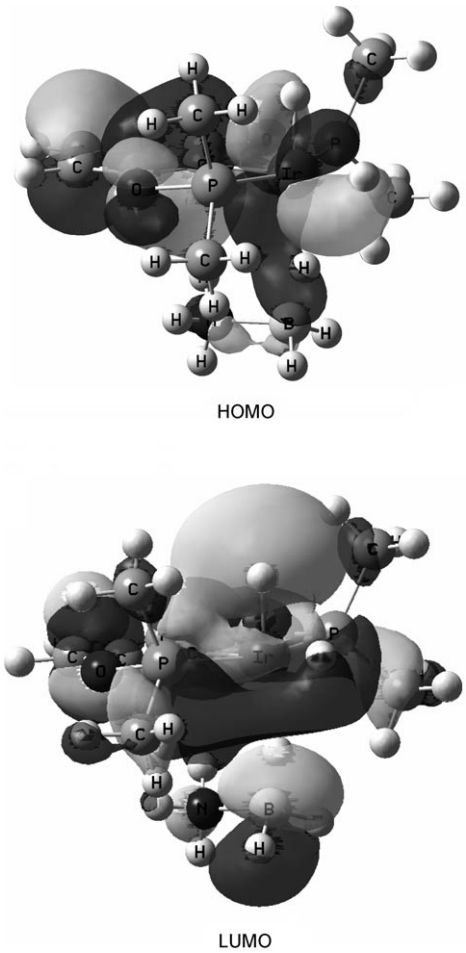

Figure 3. Frontier molecular orbitals of intermediate **6**.

Received: June 29, 2007
Published online: September 20, 2007

Keywords: ammonia–borane · dehydrogenation · density functional calculations · hydrogen storage · iridium

[1] a) *The Hydrogen Economy: NRC and NAE*, The National Academies Press, Washington, DC, **2004**; b) The Hydrogen Initiative; http://www.aps.org/public_affairs/index.cfm; The American Physical Society, **2004**; c) Basic Research Needs for the Hydrogen Economy; http://www.sc.doe.gov/bes/reports/files/NHE_rpt.pdf; Office of Science at the U.S. DOE, **2004**.
[2] C. A. Jaska, K. Temple, A. J. Lough, I. Manners, *J. Am. Chem. Soc.* **2003**, *125*, 9424–9434.
[3] C. A. Jaska, I. Manners, *J. Am. Chem. Soc.* **2004**, *126*, 9776–9785.
[4] Y. Chen, J. L. Fulton, J. C. Linehan, T. Autrey, *J. Am. Chem. Soc.* **2005**, *127*, 3254–3255.
[5] F. H. Stephens, R. T. Baker, M. H. Matus, D. J. Grant, D. A. Dixon, *Angew. Chem.* **2007**, *119*, 760–763; *Angew. Chem. Int. Ed.* **2007**, *46*, 746–749.

[6] M. C. Denney, V. Pons, T. J. Hebden, D. M. Heinekey, K. I. Goldberg, *J. Am. Chem. Soc.* **2006**, *128*, 12048 – 12049.
[7] R. J. Keaton, J. M. Blacquiere, R. T. Baker, *J. Am. Chem. Soc.* **2007**, *129*, 1844 – 1845.
[8] T. J. Clark, K. Lee, I. Manners, *Chem. Eur. J.* **2006**, 12, 8634 – 8648.
[9] M. E. Bluhm, M. G. Bradley, R. Butterick, U. Kusari, L. G. Sneddon, *J. Am. Chem. Soc.* **2006**, *128*, 7748 – 7749.
[10] K. Zhu, P. D. Achord, X. Zhang, K. Krogh-Jespersen, A. S. Goldman, *J. Am. Chem. Soc.* **2004**, *126*, 13044 – 13053.
[11] K. Krogh-Jespersen, M. Czerw, K. Zhu, B. Singh, M. Kanzelberger, N. Darji, P. D. Achord, K. B. Renkema, A. S. Goldman, *J. Am. Chem. Soc.* **2002**, *124*, 10797 – 10809.
[12] K. Krogh-Jespersen, M. Czerw, M. Kanzelberger, A. S. Goldman, *J. Chem. Inf. Comput. Sci.* **2001**, *41*, 56 – 63.
[13] K. Krogh-Jespersen, M. Czerw, N. Summa, K. B. Renkema, P. D. Achord, A. S. Goldman, *J. Am. Chem. Soc.* **2002**, *124*, 11404 – 11416.
[14] I. Gottker-Schnetmann, P. S. White, M. Brookhart, *J. Am. Chem. Soc.* **2004**, *126*, 1804 – 1811.
[15] I. Gottker-Schnetmann, P. S White, M. Brookhart, *Organometallics* **2004**, *23*, 1766 – 1776.
[16] A. S. Goldman, A. H. Roy, Z. Huang, R. Ahuja, W. Schinski, M. Brookhart, *Science* **2006**, *312*, 257 – 261.
[17] S. Li, M. B. Hall, *Organometallics* **2001**, *20*, 2153 – 2160.
[18] S. Niu, M. B. Hall, *J. Am. Chem. Soc.* **1999**, *121*, 3992 – 3999.
[19] Gaussian 03, revision C.02, M. J. Frisch, et al. (see Supporting Information, Gaussian, Inc., Wallingford, CT, **2004**.
[20] M. Cossi, N. Rega, G. Scalmani, V. Barone, *J. Comput. Chem.* **2003**, *24*, 669 – 681.
[21] I. Gottker-Schnetmann, D. M. Heinekey, M. Brookhart, *J. Am. Chem. Soc.* **2006**, *128*, 17114 – 17119.
[22] M. Shimoi, S. Nagai, M. Ichikawa, Y. Kawano, K. Katoh, M. Uruichi, H. Ogino, *J. Am. Chem. Soc.* **1999**, *121*, 11704 – 11712.
[23] R. T. Baker, D. W. Ovenall, J. C. Calabrese, S. A. Westcott, N. J. Taylor, I. D. Williams, T. B. Marder, *J. Am. Chem. Soc.* **1990**, *112*, 9399 – 9400.
[24] K. W. Boddeker, S. G. Shore, R. K. Bunting, *J. Am. Chem. Soc.* **1966**, *88*, 4396 – 4401.
[25] Y. Luo, K. Ohno, *Organometallics* **2007**, *26*, 3597 – 3600.

